

Accelerator Department  
BROOKHAVEN NATIONAL LABORATORY  
Associated Universities, Inc.  
Upton, New York 11973

ISABELLE Project

Technical Note No. 331

SENSITIVITY OF THE CABLE MAGNET TO VARIATIONS  
IN DESIGN PARAMETERS

R. Fernow

December 3, 1981

We examined the influence of small parameter errors on the multipole structure of the cable dipole magnets. This note considers circular errors in the straight section of the magnet.

## 1. General Description of Multipoles

Many people (myself included), do not have an intuitive feeling for what it means for a magnet to have, for example, a large  $a_3$  component or a small  $b_2$  component in the decomposition of its field. For this reason let me briefly present a general description of multipoles that I have found useful in understanding what the presence of various terms mean. The experts should feel free to proceed to section 2.

The field at the point  $(r, \phi)$  within the aperture of the magnet can be decomposed in two dimensional cylindrical coordinates as

$$B_r = \sum_{n=0}^{\infty} r^n (b_n \sin(n+1)\phi + a_n \cos(n+1)\phi) \quad (1)$$
$$B_\phi = \sum_{n=0}^{\infty} r^n (b_n \cos(n+1)\phi - a_n \sin(n+1)\phi)$$

The coefficients  $a_n$  and  $b_n$  in these expansions are the multipoles which can be expressed in terms of the current density  $j(r, \phi)$  in the coils as

$$b_n = \frac{\mu_0}{2\pi} \iint \frac{j(r, \phi) \cos(n+1)\phi \left[ 1 + \left(\frac{r}{R}\right)^{2(n+1)} \right] r dr d\phi}{r^{n+1}} \quad (2)$$
$$a_n = \frac{-\mu_0}{2\pi} \iint \frac{j(r, \phi) \sin(n+1)\phi \left[ 1 + \left(\frac{r}{R}\right)^{2(n+1)} \right] r dr d\phi}{r^{n+1}}$$

where  $R$  is the inner radius of an infinite iron yoke.

The presence or absence of a particular multipole depends on the symmetry of  $j(r, \phi)$  with respect to  $\phi$ . The radial dependence of  $j(r, \phi)$  can influence the magnitude of any non-zero terms.

The multipoles differ because of the different trigonometric functions which sample the current density function.

The current density within a coil block is assumed to have the form  
(cf. H. Hahn, TN305)

$$\langle j \rangle = \frac{\bar{r} I}{\bar{t} \Delta r^2} \left( \frac{1}{r_o} + \frac{1}{r_i} \right) = \frac{I}{\bar{t}} \frac{\bar{r}^2}{r_o(r_o - r_i)}$$

$$j(r, \phi) = \frac{\bar{r} I}{\bar{t} (r_o - r_i)} \frac{1}{r} \quad (3)$$

where  $I$  is the current,  $r_i$ ,  $r_o$  and  $\bar{r}$  are the inner, outer, and mean radii of the coil, and  $\bar{t}$  is the average thickness of a turn.

The symmetry properties of the magnet are determined by the sampling integrals

$$B_n(\phi) = \int_0^{2\pi} j(\phi) \cos(n+1)\phi \, d\phi \quad (4)$$

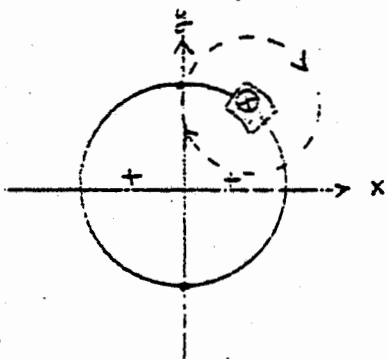
$$A_n(\phi) = \int_0^{2\pi} j(\phi) \sin(n+1)\phi \, d\phi \quad (5)$$

where  $j(\phi)$  is  $\pm 1$  for  $\phi$  in the current block and 0 otherwise.

The sign convention for Eqs. (2,4,5) were determined in the following manner. Equation (1) implies that the y component of the field on the midplane

is given by

$$B_y = \sum_{n=0}^{\infty} b_n x^n \quad (6)$$



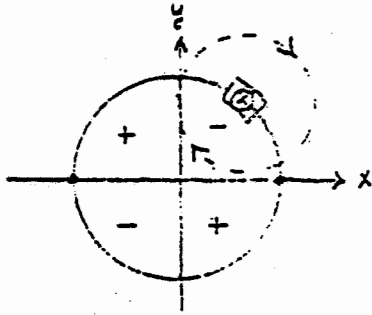
We require that the main field component be along  $+y$ . This means that a current block in the first

quadrant has current flowing into the paper. The function  $B_0$  has poles at  $90^\circ$  and  $270^\circ$ . Since  $B_y$  is positive in the figure  $b_0$  must also be positive. This means that the function  $B_0$  must be positive in the first quadrant. We can construct a picture of the multipole sampling by alternating the sign of the sampling function each time we pass a pole and then reversing all the signs on the left hand side of the magnet to take into account the reversal of current

direction on that side. Such sampling figures for multipoles with  $n \leq 6$  are shown in Figure 1. It also follows from Eq. (1) that

$$B_x = \sum_{n=0}^{\infty} a_n x^n \quad (7)$$

If we consider  $B_x$  at the origin then only  $a_0$  can contribute. The poles of the  $a_0$  sampling function are at  $0^\circ$  and  $180^\circ$ . A current block in the first quadrant



will generate a negative  $B_x$ , which implies that  $a_0$  must be negative. This requires that the first quadrant sampling function be negative. The signs of the remaining three quadrants are determined as above.

(I) Left-right symmetry

In this case we can write the current density as

$$j(\phi) = -j(\pi - \phi) \quad (8)$$

The minus sign arises since the current in the right and left halves of the magnet travels in opposite directions. We will explicitly calculate the effect on  $B_n$  to demonstrate the technique. Substitute (8) into (4) and adopt the notation  $\bar{n} = n+1$

$$B_n(\phi) = \int_{-\pi/2}^{\pi/2} j(\phi) \cos \bar{n}\phi \, d\phi + \int_{\pi/2}^{3\pi/2} (-) j(\pi-\phi) \cos \bar{n}\phi \, d\phi \quad (9)$$

If we made the substitution  $\theta = \pi - \phi$  in the second integral we get

$$\begin{aligned} I_2 &= - \int_{\pi/2}^{-\pi/2} j(\theta) \cos \bar{n}(\pi-\theta) (-d\theta) \\ &= - \int_{-\pi/2}^{\pi/2} j(\theta) \cos \bar{n}\pi \cos \bar{n}\theta \, d\theta \end{aligned}$$

Substituting back into (9) gives

$$\begin{aligned}
 B_n(\phi) &= \int_{-\pi/2}^{\pi/2} j(\phi) \cos n\phi \left(1 - \cos(n+1)\pi\right) d\phi \\
 &= 2 \int_{-\pi/2}^{\pi/2} j(\phi) \cos n\phi d\phi && (n \text{ even}) \\
 &= 0 && (n \text{ odd})
 \end{aligned} \tag{10}$$

Thus we see that the presence of odd  $b_n$  terms reflect a left-right asymmetry in the current density distribution.

Similarly if we substitute (8) into (5) we find that

$$\begin{aligned}
 A_n(\phi) &= 2 \int_{-\pi/2}^{\pi/2} j(\phi) \sin n\phi d\phi && (n \text{ odd}) \\
 &= 0 && (n \text{ even})
 \end{aligned} \tag{11}$$

It follows that even  $a_n$  terms also indicate that the magnet doesn't have left-right symmetry.

## (II) Up-down symmetry

If a coil is up-down symmetric we must have

$$j(\phi) = j(-\phi) \tag{12}$$

Substituting back into (4) and (5) we find that

$$\begin{aligned}
 B_n(\phi) &= 2 \int_0^{\pi} j(\phi) \cos n\phi d\phi && (\text{all } n) \\
 A_n(\phi) &= 0 && (\text{all } n)
 \end{aligned} \tag{13}$$

We see that the presence of any  $a_n$  term would indicate an up-down asymmetry.

(III) Parity symmetry

Finally let us consider the symmetry

$$j(\phi) = -j(\pi+\phi) \quad (14)$$

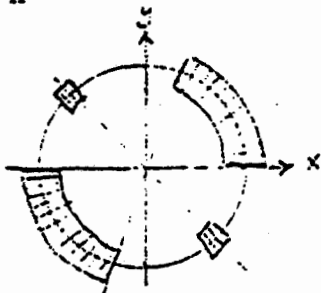
This symmetry would arise if the magnet were constructed from identical (but possibly asymmetric) coil halves.

We find that

$$\begin{aligned} B_n(\phi) &= 2 \int_0^\pi j(\phi) \cos n\phi \, d\phi && (n \text{ even}) \\ &= 0 && (n \text{ odd}) \end{aligned} \quad (15)$$

$$\begin{aligned} A_n(\phi) &= 2 \int_0^\pi j(\phi) \sin n\phi \, d\phi && (n \text{ even}) \\ &= 0 && (n \text{ odd}) \end{aligned} \quad (16)$$

This case shows that, although the presence of an odd  $a_n$  term indicates an up-down asymmetry in the magnet, it doesn't follow that the absence of odd  $a_n$  terms indicates that the magnet is up-down symmetric. As an example



consider the following current distribution which is grossly up-down asymmetric but which has all odd  $a_n$  equal 0 since it has parity symmetry.

These symmetry considerations lead naturally to dividing the multipoles into four classes.

(1) Even  $b_n$ . These are the allowed terms. We see that  $b_0$  is sampled positively everywhere meaning that all the current density contributes to the dipole field. The size of the sextupole ( $b_2$ ) term depends on the relative amount of current density within  $\pm 30^\circ$  of the midplane as compared to the current density outside this region.

(2) Odd  $a_n$ . This is the most likely class of forbidden terms which would not be present in a perfectly symmetric magnet. We see that these terms can arise if the current density is not symmetric up and down with respect to the midplane. These terms will be present if, for example, the two coil halves have different sizes.

(3) Odd  $b_n$ . These forbidden terms reflect a left-right asymmetry in the magnet. Left-right asymmetries are more unlikely than up-down ones but could arise if, for example, the molding fixture or pusher pieces were asymmetric.

(4) Even  $A_n$ . We have seen that these terms are forbidden for both left-right and up-down symmetric magnets. It follows that if these terms are present the current distribution must be both left-right and up-down asymmetric. However, these terms may be equal in importance to the odd  $b_n$  terms since they are allowed by the parity symmetry.

## 2. Magnet Design

A cross section of the current ISABELLE dipole design (R. Palmer, TLM-22) is shown in Fig. 2. The design values for the iron enhancement factors  $E_n$  are given in Table 1 along with the design values of the multipoles. In this and the following tables we will list the quantity  $b_0$  itself but express the other multipoles in the form

$$b_n' = \frac{b_n}{b_o} (4.4 \text{ cm})^n \times 10^4$$

$$a_n' = \frac{a_n}{b_o} (4.4 \text{ cm})^n \times 10^4$$

(17)

### 3. Radial Variations

In this section we will examine radial changes in the current distribution, keeping the azimuthal distribution fixed at the design values. We first consider the influence of the radial dependence of the current density on the multipoles. The current density given in Eq. (3) is strictly valid for a rectangular cable laid around a circle. It is also valid for a keystoneed cable if the wire density within the cable falls off like  $1/r$ . Cross sections cut through the cable show that this is approximately true. A true monolithic keystoneed cable on the other hand should have the current density

$$j(r, \phi) = \frac{I}{\bar{r}(r_o - r_i)} \quad (18)$$

Presumably the actual current density distribution lies somewhere between Eqs. (3) and (18). In order to see how sensitive our results are to the form of  $j(r)$  we have recalculated the radial integrals using Eq. (18). The shifts in the multipoles are given in Table 2. The largest effect is on the sextupole but no shift is very significant. We conclude that we are not sensitive to the exact form of  $j(r)$  and exhibit multipoles calculated from Eq. (3) in the remainder of this report.

We have considered five perturbations to the radii given in Fig. 2.

- (1) Increase  $\bar{r}_{out}$  by 5 mils. Keep  $\bar{r}_{in}$ ,  $\Delta r$ , and  $R$  at the design values ( $\Delta r$  is the radial width of the cable).

- (2) Increase  $\bar{r}_{in}$  by 5 mils keeping  $\bar{r}_{out}$ ,  $\Delta r$ , and  $R$  at design values.
- (3) Increase  $\Delta r$  by 4 mils keeping  $\bar{r}_{in}$ ,  $\bar{r}_{out}$ , and  $R$  at design values.
- (4) Increase  $R$  by 5 mils keeping  $\bar{r}_{in}$ ,  $\bar{r}_{out}$ , and  $\Delta r$  at design values.
- (5) Decrease  $R$  by 5 mils keeping  $\bar{r}_{in}$ ,  $\bar{r}_{out}$ , and  $\Delta r$  at design values.

The results are given in Table 2. We see that the multipoles are relatively insensitive to reasonable variations in the radii. The largest effects occur in the sextupole term. The most sensitive parameter appears to be the mean radius of the inner coil.

#### 4. Azimuthal Variations

In this section we will consider various perturbations to the azimuthal current distribution. The radial dependence is fixed at the design value. We first considered the effect of using large current blocks in the azimuthal integral. The actual current distribution consists of many thin wedges of conductor separated by insulation layers. The program was modified to sum over individual conductors. It was assumed that there are 4 mils of insulation on each side of the conductor when it is compressed in the magnet. We found that the large block approximation was extremely accurate. The largest deviation occurred in  $b_2'$ , which decreased by .01. The reason for the good accuracy in the approximation is that, even though the fraction of the azimuth that is integrated over is increased, the current density is proportional to  $1/\bar{r}$  and  $\bar{r}$  also increases.

Now consider the changes in the multipoles that arise from errors in angular positions or wedge sizes. Figure 3 illustrates the parameters that have been varied. All of the perturbations listed below involve a change of 8 mils which corresponds to  $.167^\circ$  for the inner coil and  $.150^\circ$  for the outer coil.

(1) Post angle. The inner and outer post angles have been separately increased by 8 mils. Note that this error is only introduced at the angle indicated. Results for symmetric errors can be deduced from the symmetry relations in Section 1. It was assumed that the upper post angle, the copper wedge size, and midplane shim size remain fixed at their design values and the coil blocks share the 8 mil compression proportionately. The results are indicated in Table 3.

(2) Midplane shim size. The inner and outer midplane shim sizes have been separately increased by 8 mils.\* It was assumed that the post angles, and copper wedge sizes remain fixed at the design value and the coil blocks share the compression proportionately. The results are given in Table 4. Note that this perturbation decreases all the  $b'_n$  and does not affect the  $a'_n$

(3) Copper wedge size. One of the inner or outer copper wedge sizes has been increased by 8 mils. It was assumed that the post angles, midplane shim size and other copper wedge sizes remained fixed at the design values, and that the coil blocks share the compression proportionately. The results are shown in Table 5.

\* that is 4 mils were added to the wedge above the midplane and 4 mils were added below the midplane

(4) Copper wedge angle. The angular position of one of the inner or outer copper wedges has been moved 8 mils closer to the midplane. The post angles, shim and wedge sizes, and wedge positions in the other coil are fixed at their design values. The coil block below the wedge is expanded by the 8 mils while the 3 coil blocks above the wedge are compressed proportionately. The results are shown in Table 6.

(5) Midplane shim angle. The angular position of the midplane shim of one of the coils is increased by 8 mils toward the upper post. The post angles, shim and wedge sizes, and the other midplane shim are fixed at their design values. The 2 coil blocks above and below the midplane are compressed or expanded proportionately. The results are given in Table 7. Note that this error has practically no effect on the  $b'$  terms but can fairly easily generate a large  $a'$  term.

Table 1. Design Enhancements and Multipoles

	Inner Coil	Outer Coil	$b'_n$
$n$	$E_n$	$E_n$	
0	1.645	1.809	15.1060
1	1.417	1.655	0
2	1.269	1.530	-11.02
3	1.174	1.429	0
4	1.112	1.347	- 2.56
5	1.072	1.281	0
6	1.047	1.228	.11
7	1.030	1.184	0
8	1.019	1.149	- .19

Table 2. Multipole Changes for Radial Perturbations

	$\Delta b_0$	$\Delta b_2'$	$\Delta b_4'$	$\Delta b_6'$	$\Delta b_8'$
Form of $j(r)$	-.0025	+.45	-.07	-.01	+.02
Increase $\bar{r}_{out}$	-.0004	-.25	+.06	+.01	-.01
Increase $\bar{r}_{in}$	-.0013	+.53	-.10	-.02	+.02
Increase $\Delta r$	+.0001	-.01	.00	.00	.00
Increase R	-.0073	-.19	+.03	+.01	.00
Decrease R	+.0073	+.19	-.03	.00	+.01

Table 3. Multipole Errors from Post Angle Error

n	Inner Post		Outer Post	
	$\Delta b'_n$	$\Delta a'_n$	$\Delta b'_n$	$\Delta a'_n$
0	+0.0033	-4.21	+0.0012	-2.77
1	+2.47	-1.11	+1.26	-2.06
2	+ .62	+ .93	+1.02	- .82
3	- .51	+ .60	+ .53	- .09
4	- .36	- .12	+ .15	+ .12
5	+ .05	- .22	- .02	+ .09
6	+ .12	- .02	- .05	+ .02
7	+ .02	+ .06	- .03	- .02
8	- .03	+ .02	.00	- .02

Table 4. Multipole Errors from Midplane Shim Size

	Inner Shim	Outer Shim
n	$\Delta b'_n$	$\Delta b'_n$
0	-.0017	-.0005
1	-1.96	- .69
2	-1.61	- .70
3	- .93	- .54
4	- .46	- .35
5	- .26	- .20
6	- .18	- .11
7	- .12	- .06
8	- .07	- .03

Table 5. Multipole Errors from Copper Wedge Size

n	Inner Wedge		Outer Wedge	
	$\Delta b'_n$	$\Delta a'_n$	$\Delta b'_n$	$\Delta a'_n$
0	+ .0027	-4.14	+ .0003	-2.09
1	+2.31	-1.48	+ .36	-1.89
2	+ .90	+ .73	+ .40	-1.16
3	- .31	+ .78	+ .35	- .56
4	- .46	+ .05	+ .25	- .19
5	- .09	- .27	+ .15	- .02
6	+ .14	- .13	+ .08	+ .04
7	+ .09	+ .05	+ .03	+ .04
8	- .01	+ .07	+ .01	+ .03

Table 6. Multipole Errors from Copper Wedge Angle

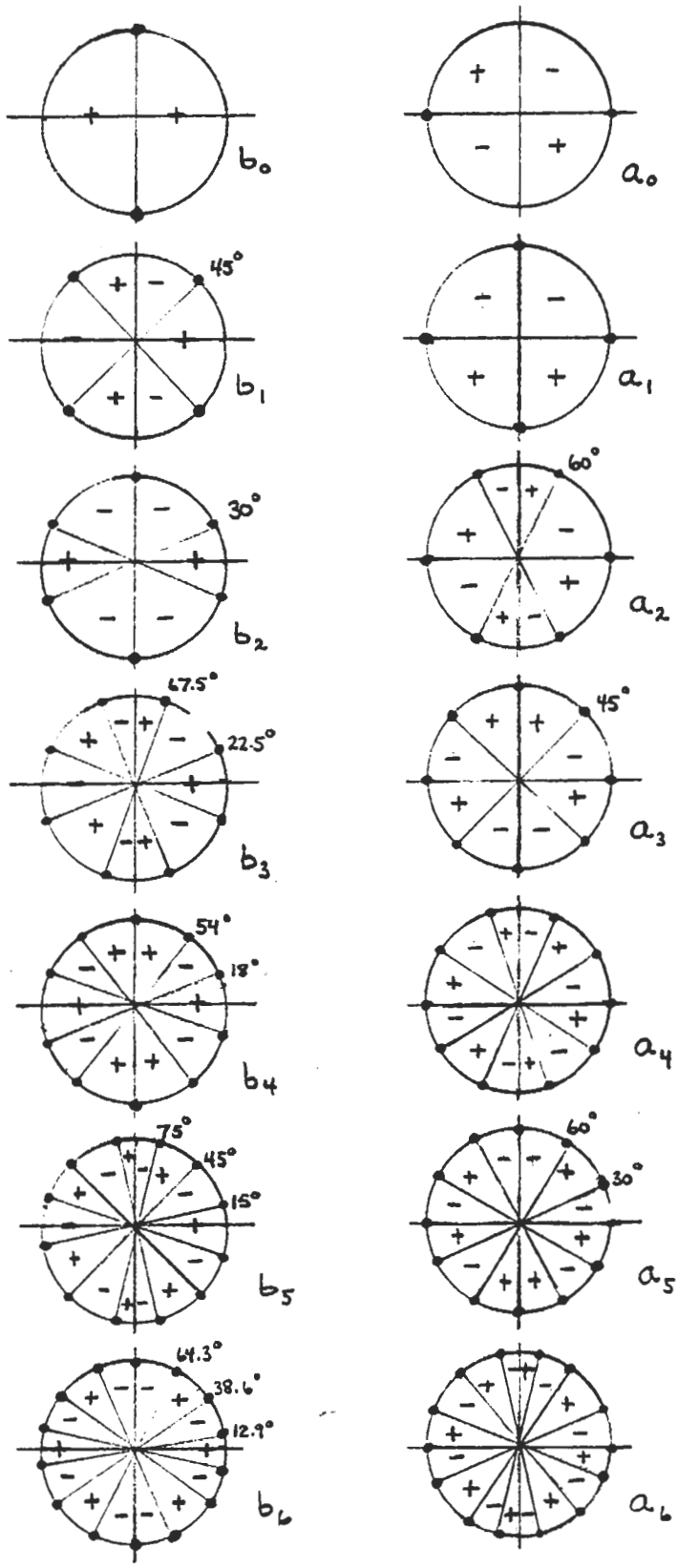
n	Inner Wedge		Outer Wedge	
	$\Delta b'_n$	$\Delta a'_n$	$\Delta b'_n$	$\Delta a'_n$
0	+0.0031	-4.31	+0.0008	-2.86
1	+2.47	-1.34	+ .94	-2.35
2	+ .79	+ .56	+ .86	-1.20
3	- .43	+ .72	+ .55	- .39
4	- .43	- .04	+ .26	- .03
5	- .02	- .26	+ .09	+ .06
6	+ .14	- .08	+ .01	+ .05
7	+ .06	+ .06	- .01	+ .02
8	- .02	+ .05	.00	+ .01

Table 7. Multipole Errors from Midplane Shim Angle

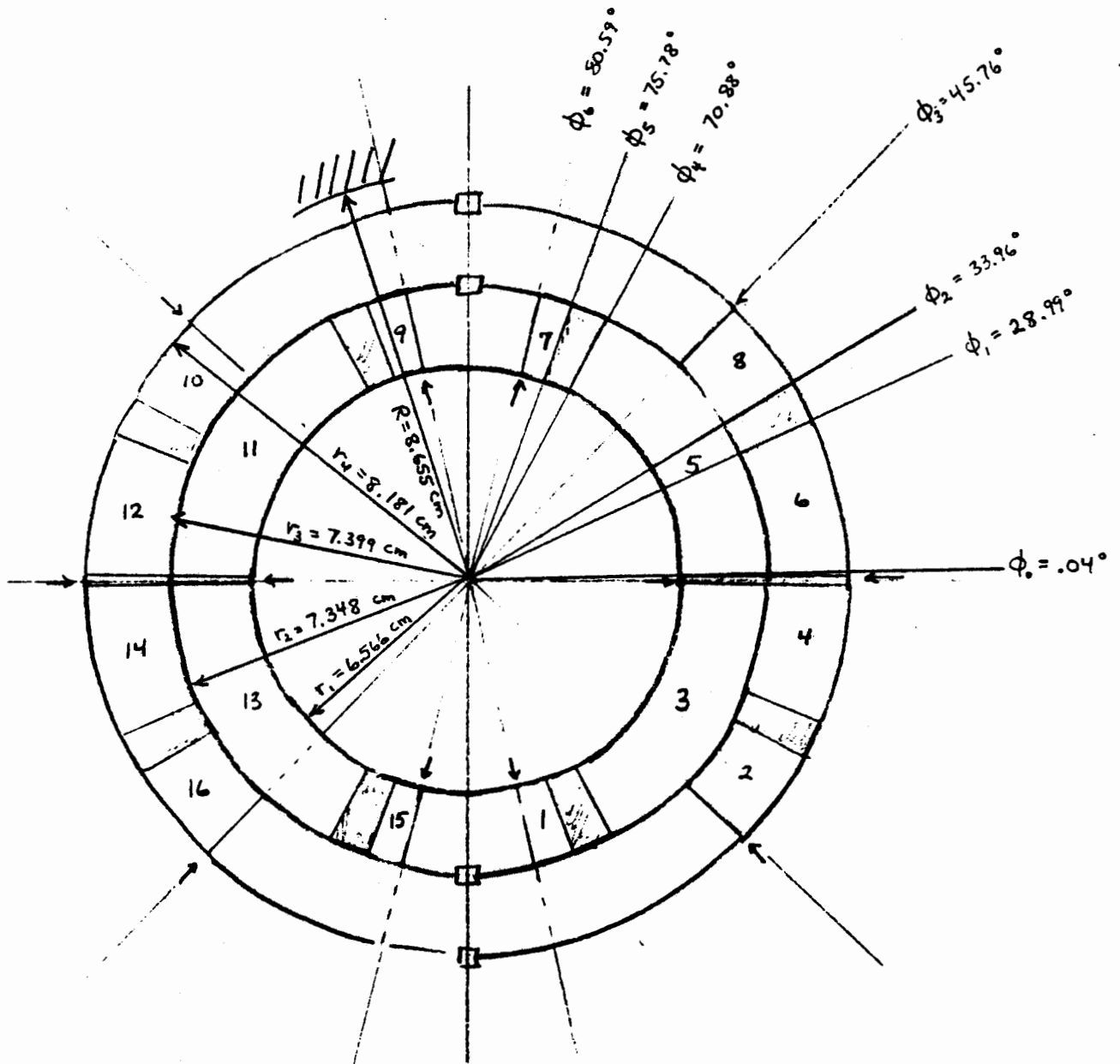
n	Inner Shim		Outer Shim	
	$\Delta b'_n$	$\Delta a'_n$	$\Delta b'_n$	$\Delta a'_n$
0	-.0001	-4.91	.0000	-2.89
1	- .11	-3.40	-.04	-2.60
2	- .04	-1.21	-.04	-1.62
3	+ .01	- .17	-.02	- .82
4	+ .01	.00	-.01	- .36
5	.00	- .06	.00	- .14
6	- .01	- .07	.00	- .05
7	.00	- .04	.00	- .02
8	+ .01	- .01	.00	- .01

# Current Sampling Diagrams

Figure 1

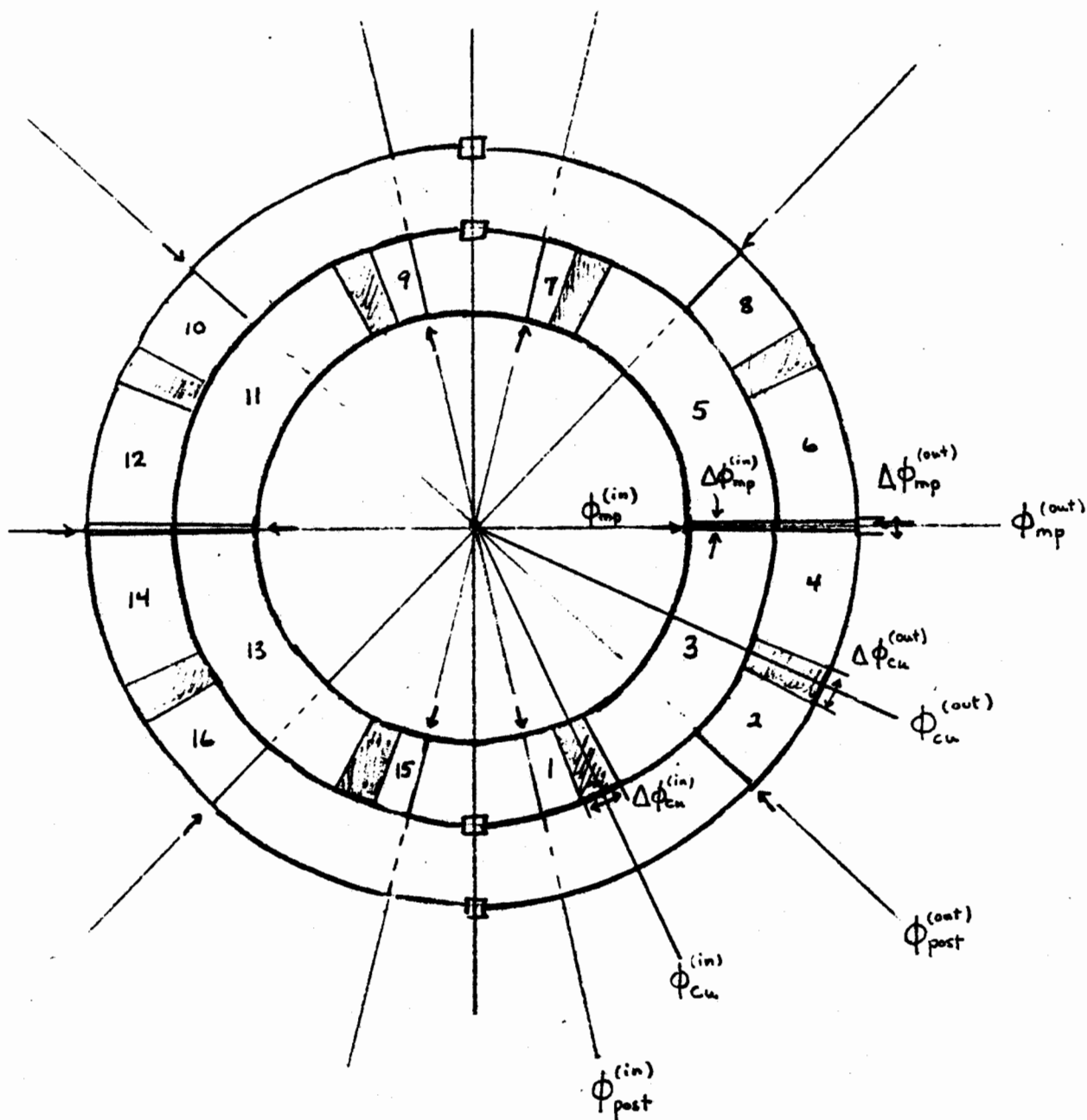


Design Parameters  
Figure 2



Azimuthal parameters

Figure 3



Bldg. 911

H. Fadem  
J. Grisoli  
H.J. Halama  
D. Lazarus  
Y. Lee  
D. Lowenstein  
M. Smith (1) plus  
one for each author(s) file  
J.R. Sanford  
D.H. White

Bldg. 902

M.Q. Barton  
H. Foelsche  
H. Hahn  
R.I. Louttit  
R.B. Palmer  
E.P. Rohrer  
J. Spiro

Bldg. 510

N. Samios  
R.P. Shutt  
H. Gordon  
T.F. Kycia  
L. Leipuner  
S. Lindenbaum  
S. Ozaki  
S. Protopopescu  
M. Sakitt  
I. Stumer  
T.L. Trueman

Bldg. 725

L. Blumberg for  
NSLS Library

W.R. Casey, 535A  
D.G. Dimmler, 535

H. Becker  
E. Bleser  
R. Engelmann  
C. Goodzeit  
A. Greene  
S. Kahn  
J. Kaugerts  
H. Kirk  
R. Palmer  
D. Rahm  
R. Shutt  
H. Hsieh  
M. Tannenbaum  
P. Wanderer

/pmb